MCF-based quantum CDC-ROADM architecture with multi-granularity switching function

Ziliang Xu, Yongmei Sun*, Weiwen Kong, Yaoxian Gao

The State Key Laboratory of Information Photonics and Optical Communications, Beijing University of Posts and Telecommunications, Haidian District, Beijing, 100876, China.

**ymsun@bupt.edu.cn*

***Abstract*—We propose a novel multi-core fiber (MCF) -based quantum CDC-ROADM (MCF-QROADM) with multi-granularity switching function. MCF-QROADM uses MCFs as the fibers of the port to improve transmission capacity. Moreover, MCF-QROADM can pass through fewer devices to achieve the function of multi-granularity switching, which can reduce the loss of the quantum signal caused by the switch node architecture, and thus increase the transmission distance of quantum signals. In addition, MCF-QROADM can achieve the function of colorless, directionless and contentionless (CDC) through the design of reasonable add and drop modules. The simulation results show that MCF-QROADM has a better performance than the existing architectures.**

Keywords—multi-core fiber, quantum key distribution, multi-granularity, ROADM

I. INTRODUCTION

The combination of quantum key distribution (QKD) [1] with one-time-pad (OTP) technology is regarded as one of the most promising technologies for the future secure communications, because QKD can significantly improve the security of information transmission. In recent years, the development of QKD has been gradually improved, and the point-to-point QKD research has made significant progress. Optical switching nodes can extend point-to-point QKD system into point-to- multipoint QKD network. In the QKD system, quantum optical switching node is the main interconnection equipment of quantum optical switching network and the main technology to expand the scale of network. Through optical network switching technology, the capacity of switching can be expanded [2], the cost of constructing quantum key distribution network can be saved, and the flexibility and reliability of network can be greatly improved.

With the increasing demand of network traffic, the transmission capacity of traditional single-core single-mode fiber (SMF) has approached Shannon limit [3]. Multi-core fiber (MCF), as a technology of Space Division Multiplexing (SDM), combined with Wavelength Division Multiplexing (WDM), can break the capacity bottleneck and significantly improve transmission capacity [4]. In addition, the co-fiber transmission of classical signal and quantum signal can reduce the cost and improve the practicality of QKD. Therefore, in the co-fiber transmission scenario based on quantum signal and classical signal dual-dimensional multiplexing, the research of optical switching technology based on QKD becomes a critical issue.

Since quantum signals are extremely weak and cannot be cloned or amplified, the switching node structure in classical optical networks is not suitable for quantum communication [5]. In order to solve this problem, in 2017, our team proposed a layered multi-granularity switching structure (LMGS) based on wavelength selective switch (WSS), which divides the switch of optical signals into three granularity: wavelength layer, wave band layer and fiber layer [6]. However, when quantum signals pass through this architecture, they may need to be transmitted up and down between different granularity layers to complete the signal switch, which will lead to excessive attenuation when quantum signals pass through this switching node. In 2020, the University of Bristol proposed a colorless and directionless (CD) quantum-switched reconfigurable optical add drop multiplexer (q-ROADM) architecture that supports flexible grids and has flexible scalability [7]. However, in this architecture, the classical signal and quantum signal co-fiber transmission will cause the quantum signal to suffer from large noise, which will lead to the decrease of QKD performance. Moreover, due to the optical fiber switch (OFS) constraint and color constraint, two QKD channels cannot be routed to the same output port, therefore, the "contentionless (C)" function cannot be achieved. The switching nodes described above all have disadvantages in improving QKD performance. In addition, the existing switching nodes for co-fiber transmission of quantum signal and classical signal are all designed based on SMF, without considering MCF.

In this paper, we propose a MCF-based quantum CDC-ROADM architecture (MCF-QROADM) with multi-granularity switching function. MCF-QROADM uses MCFs as the fibers of the port to adapt to the increasing data traffic demand and improve transmission capacity. Such MCF-QROADM uses optical switch (OS) and WSS to achieve the function of multi-granularity switching. Compared to LMGS, MCF-QROADM pass through fewer devices, which can reduce the loss of the quantum signal caused by the switch node architecture, and thus increase the transmission distance of quantum signals. Besides, MCF-QROADM uses WSSs and couplers or splitters as add and drop modules, which can achieve "contentionless" function compared to q-ROADM. Then, in the scenario of the quantum signal transmission alone or the classical signal and the quantum signal co-fiber transmission, the advantages of MCF-QROADM in increasing the transmission distance of the quantum signal or transmission capacity of signals are verified by simulation, which means that MCF-QROADM can support quantum communication better than the LMGS and q-ROADM.

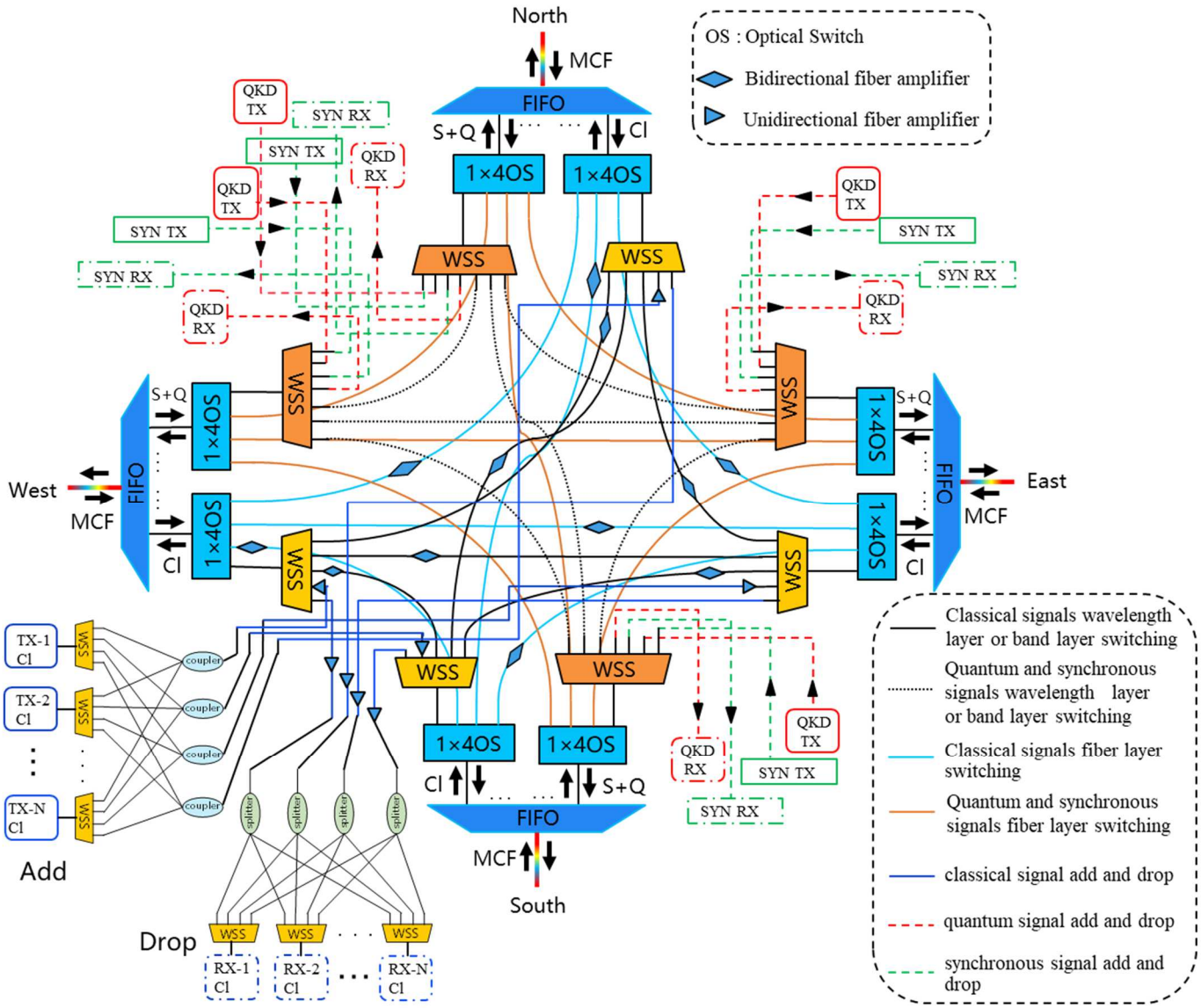

Fig. 1. The 4-degree MCF-QROADM architecture.

II. Architecture Design

A. Switching Module

Fig. 1 shows the 4-degree MCF-QROADM architecture. This architecture has the port in four directions (the number of ports can be increased or decreased as required), and the fibers of the port use MCFs. Considering that in the traditional DWDM system, the bidirectional transmission of classical signals in the fiber can save the networking costs, so we assume that the ports of this switch node architecture can be used as input ports or output ports.

In QKD systems, each user can transmit three types of signals: quantum signals, synchronous signals, and classical signals. Synchronization signals provide clock signals in the process of QKD, which is very important for quantum signal detection. In order to ensure that the quantum signal at the receiver keeps in sync with the synchronous signal of the same user, the quantum signal and the synchronous signal should always pass through the same path during the switch process. We assume that quantum signals and synchronous signals are transmitted in the same cores, while classical signals are transmitted in independent cores.

The cores of the MCF at the ports are demultiplexed through fan-in fan-out (FIFO). According to the different types of transmitted signals, the cores are divided into the cores that transmit classical signals and the cores that transmit quantum and synchronous signals. According to different switching requirements, wavelength layer or wave band layer switching

or fiber layer switching can be selected by controlling 1×4 OSs. In this paper, we employ Micro-Electro-Mechanical-Switch (MEMS) as the OS. For wavelength layer or wave band layer switching, the signals need to pass through the OS and WSS of a input port and a target output port. Since WSS can flexibly switch any wavelength, it can switch wavelength layer and wave band layer of optical signal. In addition, WSS can be dynamically configured, which greatly enhances the flexibility and intelligence of the node structure, improves the node switch ability, and reduces the complexity and cost of the node structure. For fiber layer switching, the signals only need to pass through the OS of the corresponding input and output port.

Although MCF-QROADM does not have the layered module of the traditional multi-granularity switching node architecture, it can realize the switch of signal wavelength layer, wave band layer and fiber layer through OS and WSS, which means it can realize the function of multi-granularity switching.

Moreover, in this architecture, since the FIFO is the passive device, the core port connection between any two MCF ports is fixed, so the architecture only supports signal switch between the fixed core ports. In other words, signals input from a core port can be routed to only one core port in a MCF output port.

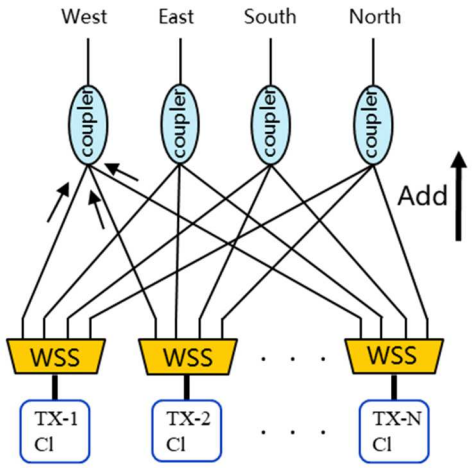

Fig. 2. The classical signal add module.

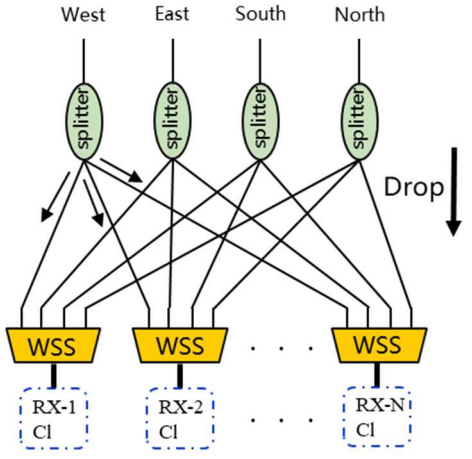

Fig. 3. The classical signal drop module.

B. *Add and Drop Modules*

In this architecture, the WSS at each core port is also equipped with local add and drop modules for classical or quantum and synchronization signals. For quantum and synchronous signals, the ports of WSS of each core port are connected with the transmitter and receiver of quantum and synchronous signals. For classical signals, the add module which is shown in Fig. 2 includes N 1×M WSS and M N×1 couplers, among which N WSSs are responsible for connecting N local signals to the ROADM system, and M N×1 couplers are responsible for routing the coupled signals to M directions respectively, where M is the degree of the switching node architecture, and M=4 in this paper. The drop module which is shown in Fig. 3 uses M 1×N splitters and N M×1 WSS, among which M 1×N splitters are used to divide optical signals in M directions into N channels, N M×1 WSS module is used to choose one output from the output signals of M splitters, and the signals which are not locally downlink can be blocked by setting WSS parameters through software. The add and drop modules designed above can avoid wavelength conflicts in the add or drop signals, so as to achieve the purpose of "no competition", which can replace M×N WSS. Therefore, the architecture has the function of colorless, directionless and contentionless (CDC). The classical signal add and drop are equipped with unidirectional fiber amplifiers as the power equalizer. In addition, considering that the architecture supports bidirectional transmission of signals during the switching process, the bidirectional fiber amplifiers are equipped on the classical signal switching link, which also plays the role of power balancing.

C. *Signal Switching Scheme*

When the services from different directions arrive at the switching node in the same time slot, we can group the services on different cores of the port to allocate wavelengths to multiple services at the same time to improve the allocation efficiency. The cores of the port in all directions can be expressed as P_j(j=1, 2, ⋯, M), where M is the degree of the switching node. Assuming that the i-th classical service in the core of the port transmitting classical service in any direction can be represented as $\{C_i, OUT_i\}$, then the i-th classical service in the core of the port can be represented as $P_j\{C_i, OUT_i\}$. Similarly, the i-th quantum service in the core of the port transmitting quantum service in any direction can be represented as $\{Q_i, S_i, OUT_i\}$, then the i-th quantum service in the core of j-port can be represented as $P_j\{Q_i, S_i, OUT_i\}$. Where C_i is the wavelength of the classical signal of the i-th classical service in the core of the port, Q_i and S_i are the wavelength of the quantum signal and synchronization signal of the i-th quantum service in the core of the port, and OUT_i is the target output core of the port of the i-th classical service or the i-th quantum service in the core of the port. The number of cores available for the target output port is M-1. In other words, for any core of the port, the service representation in classical signal core is $P_j\{C_i, OUT_i\}$; The business representation in the quantum and synchronous signal core is $P_j\{Q_i, S_i, OUT_i\}$. Assume that all wavelengths have available channels of the same wavelength in the target output core of the port (the condition of wavelength continuity is satisfied). Only when there are two cores of the port P_x and P_y （x, y∈{1, 2, ⋯, M}), when the target output port of all

services in either of the two cores of the port is the other core, which means, for any $\{C_i, OUT_i\}$ or any $\{Q_i, S_i, OUT_i\}$, when $P_x\{C_i, OUT_i\} = P_x\{C_i, P_y\}$ and $P_y\{C_i, OUT_i\} = P_y\{C_i, P_x\}$ or $P_x\{Q_i, S_i, OUT_i\} = P_x\{Q_i, S_i, P_y\}$ and $P_y\{Q_i, S_i, OUT_i\} = P_y\{Q_i, S_i, P_x\}$ is satisfied, the optical switch is controlled to make P_x and P_y for fiber layer switch; In other cases, for example, in any core of the port, if at least one service is different from the destination core of other services or at least one service needs to be routed to the local node, wavelength or wave band layer switching is performed through the control optical switch.

The above scheme can choose different switch modes according to the destination of the business in the core. Since there are fewer devices that the signal passes through the fiber layer switching than the wavelength or wave band layer switching, the fiber layer switch can not only improve the switching efficiency of the switch node, but also reduce the loss of the quantum signal caused by the switch node architecture.

III. Simulation Evaluation

In order to evaluate the performance of the proposed switching node architecture, we setup a communication link with two switching nodes on a scale with roughly the same number of switching node ports as two endpoints, as shown in Fig. 4. The switching nodes contain add and drop modules and local transmitters and receivers that can transmit and receive classical, quantum, and synchronous signals on demand. The noise level on the quantum channel is measured by a single photon detector (SPD) at the receiver and expressed in photon counts per pulse. The main parameters of the simulation QKD system are shown in Table I.

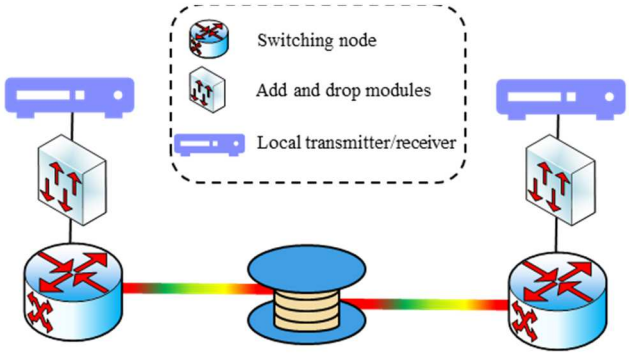

Fig. 4. The communication link with two switching nodes as two endpoints.

TABLE I. Main Parameters Used in Simulation

Parameter	Value
f_{spd} (the repetition rate of the SPD)	10 MHz
η_{spd} (detector efficiency of the SPD)	10%
p_{dark} (detection probability of dark counts of the SPD)	10^{-6}
τ_{gate} (the gate duration of the SPD)	1ns
Average number of photons per pulse	0.4
The number of cores of MCF	7

First, when the quantum signal transmission alone, the communication distance that the quantum signal can achieve when it is transmitted in the communication link with the three switching nodes as the endpoints is simulated by taking the security key rate (SKR) [8] as function of the transmission distance. The simulation results are shown in Fig. 5.

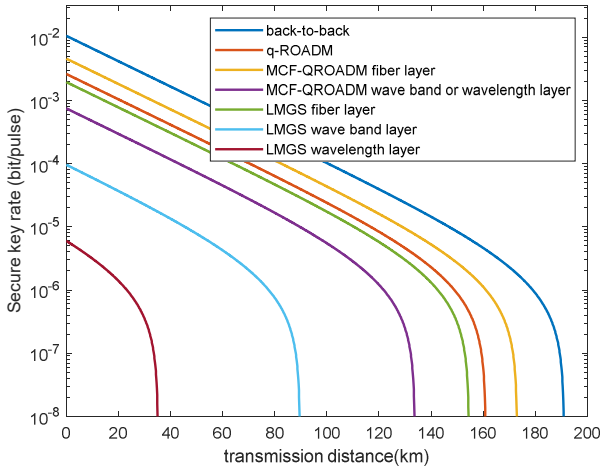

Fig. 5. The relationship between SKR and transmission distance when the quantum signal passes through different switch modes of different switching nodes in the communication link.

As can be seen from Fig. 5, the fiber layer switching of MCF-QROADM provides the best support for quantum communication, second only to back-to-back quantum communication. The wave band or wavelength layer switching of MCF-QROADM can support quantum communication better than the wave band or wavelength layer switching of LMGS.

Second, when the classical signal and the quantum signal are transmitted in the same direction through co-fiber, the communication distance that the quantum signal can achieve when it is transmitted in the communication link with MCF-QROADM and q-ROADM as the endpoints is simulated by taking the total noise photon and SKR as functions of the transmission distance. We assume that the frequency of the classical signal is f_{C1} =193.2THz, f_{C2} =193.3THz and f_{C3} =193.4THz, and the frequency of the quantum signal is f_q =193.5THz. When these signals are transmitted in the communication link with the q-ROADM as the endpoints, the fiber in the link is SMF. Because the classical signal and the quantum signal transmit in the same core, the quantum signal will be subject to the four-wave mixing noise (FWM) and spontaneous Raman scattering noise (SpRS) generated by the classical signal. When these signals are transmitted in the communication link with MCF-QROADM as the endpoints, the fiber in the link is MCF. Since the classical signal and the quantum signal are transmitted by different cores, the quantum signal will be subjected to the inter-core four-wave mixing noise (ICFWM) and inter-core Raman scattering noise (ICSpRS) generated by the classical signal.

Fig. 6 and Fig. 7 show the relationship between the number of total noise photons and SKR and the transmission distance when classical signals of different powers and quantum signals are transmitted by co-fiber in the communication link with

MCF-QROADM or q-ROADM as endpoints, respectively. As shown in Fig. 6 and Fig. 7, the quantum signal is transmitted in the communication link with MCF-QROADM as endpoints with less noise and longer transmission distance.

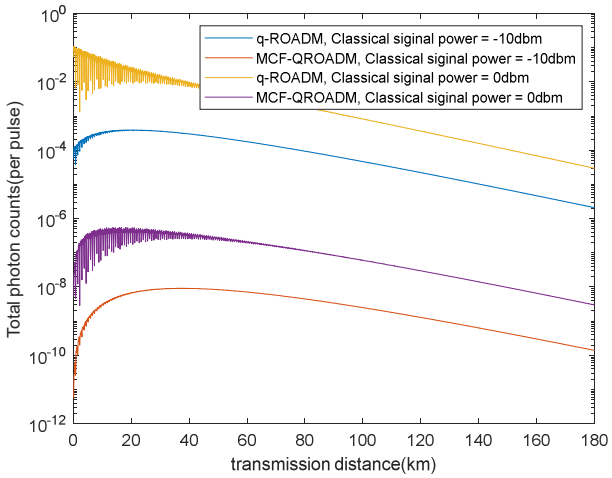

Fig. 6. The relationship between the number of total photon counts and the transmission distance when classical signals of different powers and quantum signal are transmitted by co-fiber in the communication link.

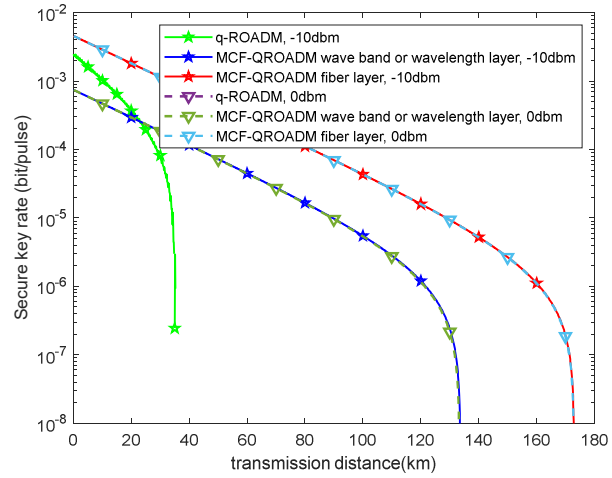

Fig. 7. The relationship between SKR and the transmission distance when classical signals of different powers and quantum signal are transmitted by co-fiber in the communication link with MCF-QROADM or q-ROADM as endpoints.

Third, based on the co-fiber transmission of classical signals and quantum signal, we increase the number of classical signals. Moreover, the same number and frequency of classical signals are placed in the remaining cores of the MCF in the communication link with MCF-QROADM as endpoints.

As shown in Fig. 5, when the classical signal power is 0dbm, the communication link with q-ROADM as the endpoints is not available. This is because the classical signal power is too large, which leads to the quantum signal is subjected to larger noise. To make the simulation effect more intuitive, we set the classical signal power to -10dbm. Moreover, we assume that 7-core fiber is used as the MCF in the communication link. When the classical signal counts (CC) is 5 and 10, the quantum bit error rate (QBER) is taken as function of the transmission distance, then we simulate the communication distance that the quantum signal can achieve when it is transmitted in the communication link with q-ROADM or MCF-QROADM as the endpoints, as shown in Fig. 8.

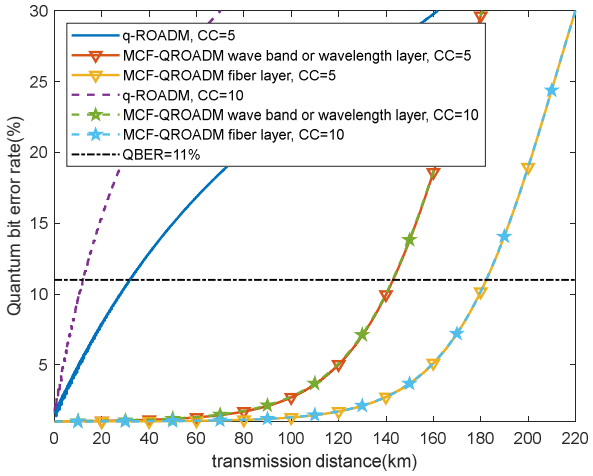

Fig. 8. The relationship between QBER and transmission distance when classical signals of different CC and quantum signal are transmitted by co-fiber in the communication link with q-ROADM or MCF-QROADM as endpoints.

When the QBER exceeds 11%, quantum communication is no longer available [9]. There is a line QBER=11% in Fig. 8 to mark the threshold available for quantum communication.

Fig. 8 shows that the communication link with q-ROADM as endpoints is more sensitive to CC. In addition, the classical signals of different CC are placed in all the six cores except the quantum cores of 7-core fiber in the communication link with MCF-QROADM as endpoints, which has little effect on the performance of the quantum signal.

Therefore, it can be concluded that the communication link with MCF-QROADM as endpoints can support more classical signals to be transmitted in each core.

Although MCFs have many more cores than SMFs, they also take up more space than SMFs. MCFs for SDM applications should have high spatial efficiency (SE) compared with a conventional SMF [10]. In SMFs or MCFs, we define the total core counts (TCC) and the classical signal core counts (CSCC) and the quantum signal core counts (QSCC). Therefore, in the communication link with q-ROADM as endpoints (in the SMF communication link), the relation TCC=CSCC=QSCC=1 is satisfied; In the communication link with MCF-QROADM as endpoints (in the MCF communication link), the relation TCC=CSCC+QSCC is satisfied.

The standard cladding diameter (CD) of the SMF is 125μm [11]. Classical signal SE (CSE) of MCF, CSE_{MCF}, and quantum signal SE (QSE) of MCF, QSE_{MCF}, are defined as:

$$CSE_{MCF}=CSCC/(\frac{\pi}{4}CD^2) \quad (1)$$

$$QSE_{MCF}=QSCC/(\frac{\pi}{4}CD^2) \quad (2)$$

Relative CSE (RCSE) and relative QSE (RQSE), which are CSE_{MCF} and QSE_{MCF} normalized by the SE of a standard SMF, respectively, SE_{SMF}, are given as:

$$RCSE = CSE_{MCF} / SE_{SMF} = CSCC \left(\frac{125}{CD}\right)^2 \quad (3)$$

$$RQSE = QSE_{MCF} / SE_{SMF} = QSCC \left(\frac{125}{CD}\right)^2$$

$$= (TCC - CSCC) \left(\frac{125}{CD}\right)^2 \quad (4)$$

The CD of 7-core fiber is 150μm [12]. When CD=150μm and TCC=7, We simulate the relationship between RCSE or RQSE and CSCC as shown in Fig. 9.

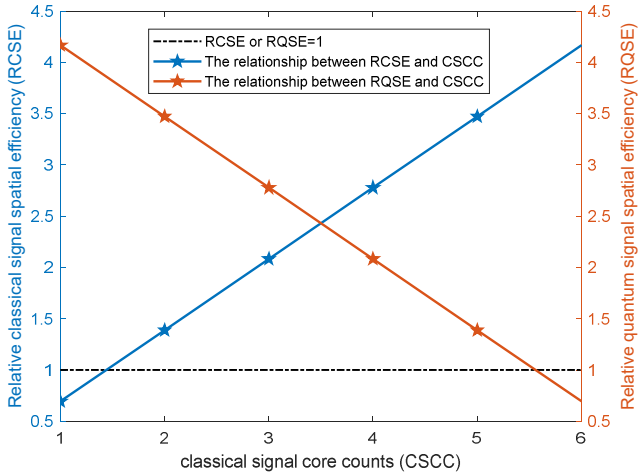

Fig. 9. The relationship between RCSE or RQSE and CSCC.

Fig. 9 shows that RCSE is in direct proportion to CSCC, while RQSR is in inverse proportion to CSCC. When CSCC=1, RCSE is less than 1; when CSCC=6, RQSE is less than 1; however, when CSCC=1, RCSE reaches the maximum; when CSCC=6, RCSE reaches the maximum. Therefore, CSCC and QSCC of MCF-QROADM can be adjusted according to the requirements of classical and quantum services, so that MCF-QROADM has higher RCSE or RQSE than q-ROADM.

In summary, in the scenario of co-fiber transmission of classical and quantum signals, MCF-QROADM can support quantum communication better than q-ROADM.

IV. Conclusion

In this paper, we proposed a MCF-based quantum CDC-ROADM architecture with multi-granularity switching function for quantum optical networks. The proposed architecture improves the flexibility and intelligence of switching nodes. In the scenario of the quantum signal transmission alone, the advantages of MCF-QROADM in improving the transmission distance of the quantum signal are verified by simulation compared to LMGS. Besides, in the scenario of the classical signal and the quantum signal co-fiber transmission, the advantages of MCF-QROADM in increasing the transmission distance of the quantum signal and transmission capacity of classical signals and higher RCSE or RQSE are verified by simulation compared to q-ROADM. Therefore, we can conclude that MCF-QROADM can support quantum communication better than the LMGS and q-ROADM, which is especially suitable for dealing with large-scale distribute requests and can be used in the QKD systems based on metropolitan area network.

Acknowledgment

This work is partly supported by National Natural Science Foundation of China (61971059).

References

[1] C. H. Bennett and G. Brassard, "Quantum cryptography: public key distribution and coin tossing," IEEE Int. Conf. on Computers, pp. 175-179, December 1984.

[2] M. Peev, A. Poppe, O. Maurhart, T. Lorunser, T. Langer and C. Pacher, "The SECOQC Quantum Key Distribution Network in Vienna," European Conference on Optical Communication, pp. 1-4, 2009.

[3] R. J. Essiambre, G. Kramer, P. J. Winzer, G. J. Foschini and B. Goebel, "Capacity Limits of Optical Fiber Networks," Journal of Lightwave Technology, vol. 28, no. 4, pp. 662-701, Februrary 2010.

[4] G. B. Xavier and G. Lima, "Quantum information processing with space-division multiplexing optical fibres," Communications Physics, vol. 3, no. 1, pp. 1–11, 2020.

[5] H. Zhang, J. Wang, K. Cui and C. Luo, "A Real-Time QKD System Based on FPGA," Journal of Lightwave Technology, Vol. 30, no.20, pp. 3226-3234, October 2012.

[6] J. Lan, Y. Sun and Y. Ji, "Experimental Realization of Multi-granularity Quantum Switch Node," Asia Communications and Photonics Conference. Optica Publishing Group, 2016.

[7] R. Wang, R. S. Tessinari, E. H. Salas, A. Bravalheri and D. Simeonidou, "End-to-End Quantum Secured Inter-Domain 5G Service Orchestration Over Dynamically Switched Flex-Grid Optical Networks Enabled by a q-ROADM," Journal of Lightwave Technology, vol. 38, no. 1, pp. 139-149, January 2020.

[8] J. Niu, Y. Sun, C. Cai and Y. Ji, "Optimized channel allocation scheme for jointly reducing four-wave mixing and Raman scattering in the DWDM-QKD system," Appl Opt, Vol. 57, no.27, pp. 7987-7996, September 2018.

[9] J. Lietzén, R. Vehkalahti and O. Tirkkonen, "A Two-way QKD Protocol Outperforming One-way Protocols at Low QBER," IEEE International Symposium on Information Theory (ISIT), pp. 1106-1111, 2020.

[10] K. Saitoh and S. Matsuo, "Multicore Fiber Technology," Journal of Lightwave Technology, vol. 34, no. 1, pp. 55-66, January 2016.

[11] P. Sillard, D. Molin, M. Bigot-Astruc, K. D. Jongh, F. Achten, A. M. Velazquez-Benitez, et al., "Low-Differential-Mode-Group-Delay 9-LP-Mode Fiber," Journal of Lightwave Technology, vol. 34, no. 2 pp. 425-430, 2016.

[12] T. Hayash, T. Taru, O. Shimakawa, T. Sasaki, E. Sasaoka, "Characterization of crosstalk in ultra-low-crosstalk multi-core fiber," Journal of Lightwave Technology, vol. 30, no. 4, pp. 583-589, 2011.